In-situ simultaneous strain and temperature measurement of adaptive composite materials using a fiber Bragg grating based sensor

Hyuk-Jin Yoon[a], Daniele Marco Costantini[b], Veronique Michaud[c], Hans Georg Limberger[b], Jan-Anders Månson[c], René Paul Salathé[b], Chun-Gon Kim[a], Chang-Sun Hong[a]
[a]Smart Structures & Composites Laboratory, KAIST, Korea
[b]Advanced Photonics Laboratory, EPFL, Switzerland
[c]Laboratoire de Technologie des Composites et Polymères, EPFL, Switzerland

ABSTRACT

An optical fiber sensor to simultaneously measure strain and temperature was designed and embedded into an adaptive composite laminate which exhibits a shape change upon thermal activation. The sensor is formed by two fiber Bragg gratings, which are written in optical fibers with different core dopants. The two gratings were spliced close to each other and a sensing element resulted with Bragg gratings of similar strain sensitivity but different response to temperature. This is due to the dependence of the fiber thermo-optic coefficient on core dopants and relative concentrations. The sensor was tested on an adaptive composite laminate made of unidirectional Kevlar-epoxy pre-preg plies. Several 150µm diameter pre-strained NiTiCu shape memory alloy wires were embedded in the composite laminate together with one fiber sensor. Simultaneous monitoring of strain and temperature during the curing process and activation in an oven was demonstrated.

Keywords: Fiber Bragg grating, fiber sensor, adaptive composite, shape memory alloy, cure monitoring.

1. INTRODUCTION

Fiber Bragg gratings (FBGs) have demonstrated a great potential for sensing applications, since their response is directly wavelength-encoded and they can easily be embedded into materials with a negligible impact on the mechanical properties of the host [1]. In particular, incorporation of FBG sensors into fiber-reinforced composite materials permits in-situ monitoring from the curing stage to their operation. A promising application consists in the control of the activation of adaptive composites, for example the strain response upon heating of materials containing shape memory alloys (SMA) [2, 3]. However, the use of FBG sensors is limited by their simultaneous dependence to strain and temperature. To overcome this cross sensitivity, a number of techniques have been proposed, most of them relying on the deconvolution of two simultaneous measurements. These methods include the dual-wavelength superimposed gratings [4], the use of first- and second-order diffraction grating wavelengths [5], FBGs in optical fibers with different dopants [6,7], hybrid Bragg grating/long-period gratings [8], dual-diameter FBGs [9], FBGs combined with EDFAs [10], FBG/EFPI combined sensors [11,12], FBGs in high-birefringence optical fibers [13], the employment of strain-free FBGs [14,15] and a combination of FBGs of different ‘type’ [16,17]. The use of a strain-free reference grating turns out to be the most efficient way to discriminate strain and temperature. On the other hand, it is not easy to implement this technique when sensors must be embedded into a host composite.

In this work, the strain and temperature into an adaptive composite laminate were simultaneously measured by using a FBG based sensor. The technique relying on the combination of two FBGs written in optical fibers with different core dopants was improved for such application. A suitable couple of optical fibers were selected, and their temperature and strain sensitivities were measured before integration. Finally, strain and temperature inside a Kevlar epoxy composite laminate with SMA wires were obtained simultaneously during curing and activation in a thermal chamber.

2. FIBER BRAGG GRATING SENSOR

A fiber Bragg grating consists in a periodic change of the core refractive index of an optical fiber and reflects light around the resonance peak wavelength defined by the following phase matching condition:

$$\lambda_B = 2n_e\Lambda \tag{1}$$

where λ_B is the Bragg wavelength, n_e is the core effective refractive index and Λ is the period of the grating. The shift of the Bragg wavelength $\Delta\lambda_B$ due to a temperature change ΔT and an axial strain ε can be expressed for a bare fiber Bragg grating as:

$$\Delta\lambda_B = \lambda_B\left[(\alpha+\xi)\Delta T + (1-p_e)\varepsilon\right] \tag{2}$$

where α is the coefficient of thermal expansion of the fiber material, ξ is the thermo-optic coefficient and p_e is the strain-optic constant [1]. The relative Bragg wavelength shift $\Delta\lambda_B/\lambda_B$ may be simply written as a function of the temperature sensitivity $K_T = \alpha+\xi$ and strain sensitivity $K_\varepsilon = 1-p_\varepsilon$ of the fiber Bragg grating:

$$\frac{\Delta\lambda_B}{\lambda_B} = K_T\Delta T + K_\varepsilon\Delta\varepsilon \tag{3}$$

The response of two fiber Bragg gratings having different temperature and/or strain sensitivities can be combined in a linear system of two equations, which can be solved for obtaining simultaneously the temperature change and strain:

$$\begin{bmatrix}\Delta T\\ \varepsilon\end{bmatrix} = \begin{bmatrix}K_{T1} & K_{\varepsilon 1}\\ K_{T2} & K_{\varepsilon 2}\end{bmatrix}^{-1}\begin{bmatrix}\dfrac{\Delta\lambda_{B1}}{\lambda_{B1}}\\ \dfrac{\Delta\lambda_{B2}}{\lambda_{B2}}\end{bmatrix} \tag{4}$$

where the subscripts 1,2 indicate the specific FBGs. Equation (4) can be rewritten in the vector form as $x = K^{-1}y$. In order to efficiently discriminate the temperature and the strain contributions, the matrix of coefficients K must be well-conditioned [18]. As a matter of fact, the relative error δx in temperature and strain is related to a Bragg wavelength change vector δy as follows:

$$\frac{\|\delta x\|}{\|x\|} \le C(K)\frac{\|\delta y\|}{\|y\|} \tag{5}$$

where $C(K) = \|K\|\|K^{-1}\|$ is the condition number of the matrix of coefficients K [19]. In order to reduce the error in the simultaneous evaluation of strain and temperature, a small condition number is desired.

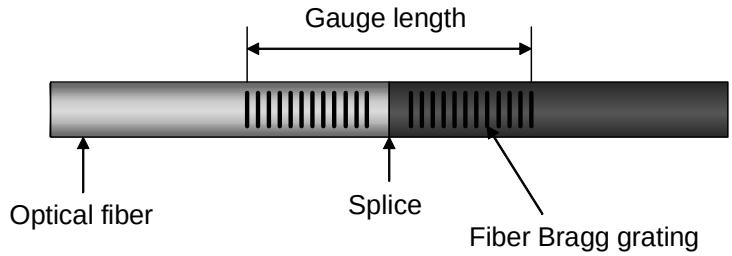

Figure 1: Design of the FBG based sensor for temperature and strain discrimination.

The thermo-optic coefficient of an optical fiber depends on the core dopants and their relative concentrations [6-7, 20]. Based on this principle, two fiber Bragg gratings fabricated in optical fibers with different core dopants are spliced close to each other to become a single and compact sensing element (Figure 1). A panel of fibers was investigated, and the

couple with the best condition number was selected. The fiber specifications and the fabrication parameters are listed in Table 1. The gratings were fabricated in these optical fibers through the phase-mask technique using a 193 nm ArF excimer laser. The same phase mask with a period of 1058.5 nm was used. The length of the gratings was of 7 mm and their reflectivity was around 50 %. Since the maximum curing temperature of the Kevlar epoxy composite material is of 140 °C, the FBG sensors were pre-annealed at 160 °C during 48 hours, in order to ensure the Bragg wavelength stability [21]. Finally, the two gratings were spliced to each other as shown in Figure 1 and formed a FBG sensor with a total gauge length of 15 mm.

Table 1: FBGs fabrication parameters (F_P: fluence per pulse; F_T: total fluence and λ_B: Bragg wavelength)

FBG	Fiber label	Fiber supplier	Core dopants [mol%]		F_P (mJ/cm^2)	F_T (J/cm^2)	λ_B (nm)
			GeO_2	B_2O_3			
1	G22	CSEM	22	-	69	1.1	1547
2	PS1500	Fibercore	10 [6]	14-18 [6]	69	5.5	1532

Temperature and strain sensitivities of the gratings were separately measured. The wavelength shift of the Bragg gratings was measured in reflection with a wavelength resolution of 0.1 pm by a tunable laser (Tunics 1550, Nettest), a photo-detector (MA9305B, Anritsu) and a wavelength meter (WA-1500, EXFO Burleigh). The relative wavelength shifts for the Bragg gratings when increasing the temperature from 25 to 140 °C with increments of 10 °C are plotted in Figure 2. Each grating was heated in an oven and the temperature measured with a resolution of ±0.1 °C by a thermocouple connected to a voltmeter (FLUKE 52k/J). The sensor response to temperature follows well a quadratic behavior. However, in order to use equation (4) for simultaneously recovering of strain and temperature, both responses are fitted to linear curve, which give slight errors in the temperature range considered. The solid and dotted lines represent the linear fitting to the experimental data for the G22 and PS1500 fibers, respectively. The G22 fiber had a temperature coefficient K_{T1} of $7.48\pm0.02 \cdot 10^{-6}\ °C^{-1}$, while the PS1500 had a coefficient K_{T2} of $6.00\pm0.01 \cdot 10^{-6}\ °C^{-1}$. The thermal expansion coefficient of the fiber material is nearly an order of magnitude lower than the thermo-optic coefficient [22]. Thus the temperature sensitivity is mainly affected by the thermo-optic coefficient, which, in turn, depends on the concentrations of GeO_2 and B_2O_3 in the core. This explains the difference in temperature sensitivity of the gratings written in the G22 and PS1500 silica fibers.

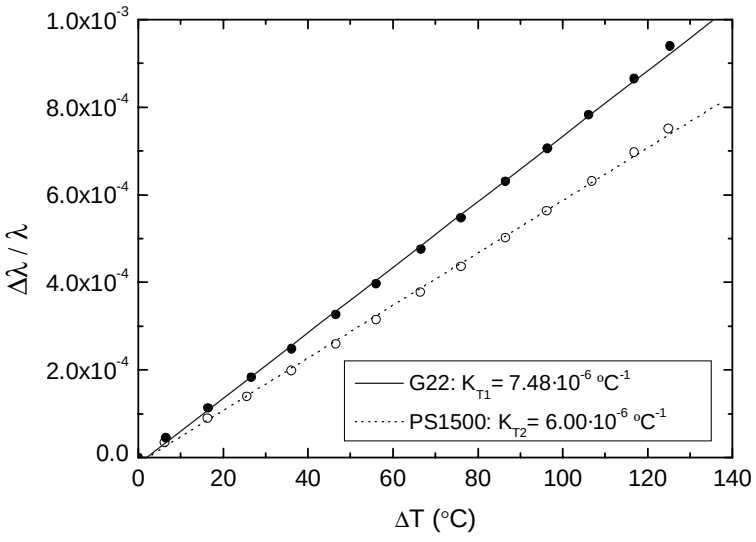

Figure 2: Relative Bragg wavelength shift as a function of temperature change for both the gratings written in the G22 and PS1500 optical fibers.

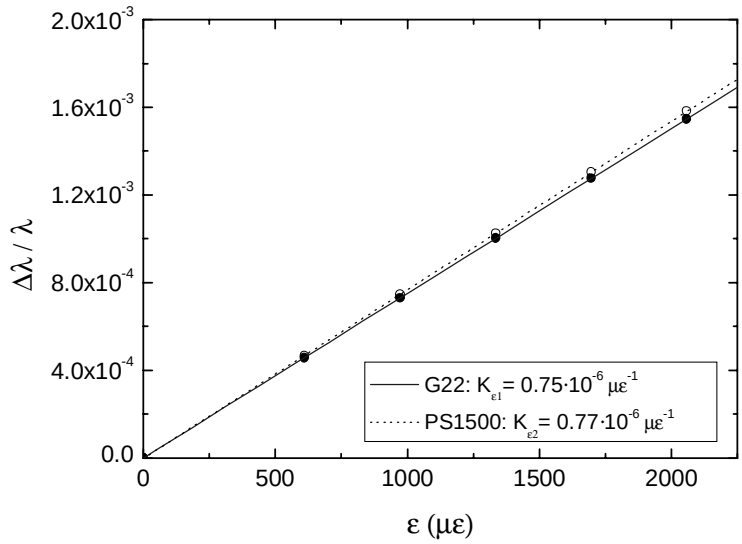

Figure 3: Relative Bragg wavelength change versus applied strain for both the gratings written in the G22 and PS1500 optical fibers.

Figure 3 shows the relative Bragg wavelength change for the two gratings when the applied strain is between 0 and 2000 $\mu\varepsilon$. The strain was induced by suspending calibrated weights to the optical fiber, and assuming a Young modulus of the fiber of 72.5 GPa [1] and a cladding diameter of 125µm. The experimental data obtained for the G22 and PS1500 grating sensors were linearly fitted. Their strain sensitivities were similar and equal to $0.75\pm0.01\cdot10^{-6}$ $\mu\varepsilon^{-1}$ and $0.77\pm0.01\cdot10^{-6}$ $\mu\varepsilon^{-1}$, respectively.

The condition number of this FBG couple was calculated and is compared in Table 2 to that of similar methods found in literature. The fiber couple from this work looks very promising as it concerns accuracy to simultaneously discriminate the temperature and strain. The condition number was improved by about 50 % with respect to similar techniques and is of the same order of magnitude of sensors combining Bragg gratings of different 'type' [16].

Table 2: Condition numbers of dual FBG sensors

Fiber 1			Fiber 2			*C(K)*	Ref.
	K_{T1} (10^{-6} °C^{-1})	$K_{\varepsilon1}$ (10^{-6} $\mu\varepsilon^{-1}$)		K_{T2} (10^{-6} °C^{-1})	$K_{\varepsilon2}$ (10^{-6} $\mu\varepsilon^{-1}$)		
Siecor SMF1528	6.48	0.75	Fibercore PS1500	5.76	0.74	147.9	[6]
Corning SMF-28	6.85	0.68	Er/Yb co-doped	5.93	0.67	146.1	[7]
B/Ge-codoped fiber (Type IA grating)	4.74	0.69	B/Ge-codoped fiber (Type IIA grating)	6.45	0.69	55.3	[16]
Fibercore SM1500 (Type I grating)	7.82	0.74	Fibercore SM1500 (Type IIA grating)	8.7	0.75	240.7	[17]
CSEM G22	7.48	0.75	Fibercore PS1500	6.0	0.77	73.8	this work

3. CURING AND ACTIVATION MONITORING OF ADAPTIVE COMPOSITE

The sensor was embedded into an adaptive composite laminate. The base composite is an unidirectional laminate made from Kevlar 29 aramid fibers and LTM217 epoxy resin pre-preg (Advanced Composites Group, UK), with about 60% volume fraction fibers. Several shape memory alloy NiTiCu wires from Furukawa with a diameter of 150µm were embedded in the laminate together with the optical fiber. These wires are martensitic at room temperature, and transform to austenite at 40°C. If they are deformed at room temperature, they will try to recover their initial shape upon heating, exerting strong recovery forces. As a consequence, strain or shape change will result in the material upon thermal activation. The specimen configuration is shown in Figure 4.

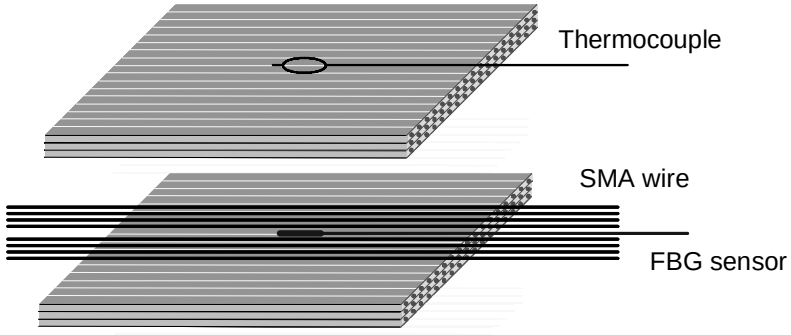

Figure 4: Direction and location of FBG and SMA wires.

The composite was stacked as $[0_2/\{0\}/0_2]_T$ on an aluminum base plate and 8 shape memory wires were laid on the neutral axis of the specimen. The FBG sensor was inserted in between the SMA wires. The SMA wires were maintained in a frame, and pre-strained to 3%. The pre-strain was maintained during the curing process. Details on the processing of the adaptive composites are given in [2, 3]. The whole assembly was then placed in a vacuum bag, and maintained under vacuum during the composite cure and post-cure. A thermocouple was attached to the bag surface close to the sample in order to have a reference temperature.

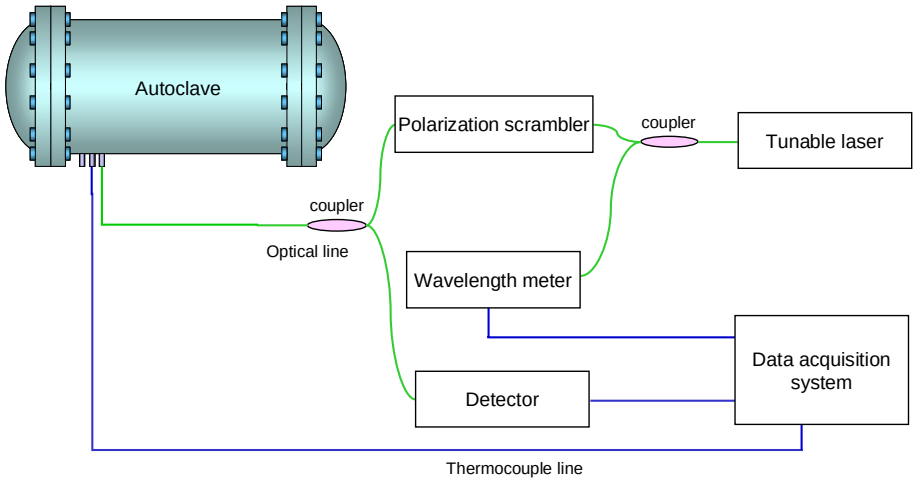

Figure 5: The experimental set-up for the cure monitoring of the composite laminate.

The experimental set-up for the cure monitoring is described in Figure 5. The light from the polarized tunable laser passes through a polarization scrambler for eliminating any birefringence effect of the Bragg grating sensors. In addition, the tunable laser light wavelength is continuously calibrated by using a wavelength meter, which has a

resolution of 0.1 *pm*. The lightsource wavelength, the light intensity reflected by the sensor and the temperature measured by the thermocouple were acquired by a computer controlled data acquisition system.

The composite laminate sample was placed in the autoclave and cured according to the LTM217 epoxy resin cycle. The temperature was increased from room temperature to 70 $^{\circ}C$ with a rate of 4 $^{\circ}C$ /min and maintained constant for 12 hours. After the first dwell, the temperature was increased to 140 $^{\circ}C$ and the heating rate was set to 20 $^{\circ}C$ /hour. After the second dwell, the temperature was lowered back to room temperature. The total cure cycle was of 24 hours with two temperature steps. During curing both the internal strain and the temperature were recorded simultaneously according to equation (4), as shown in Figure 6.

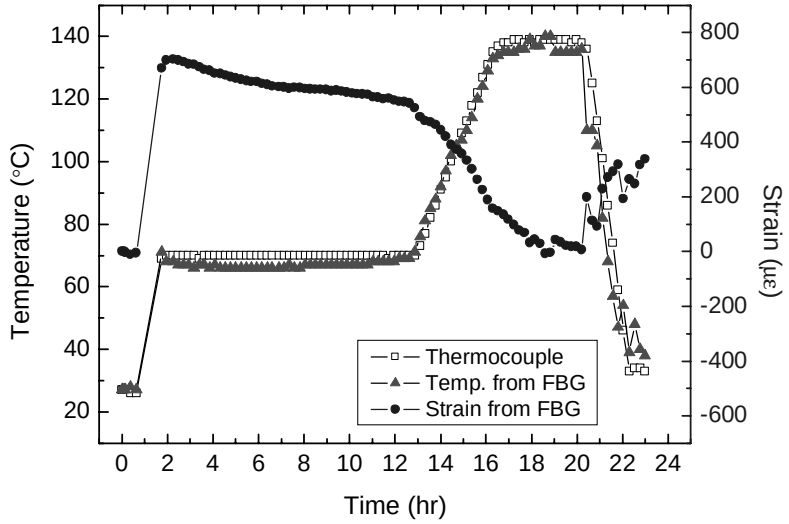

Figure 6: Strain and temperature measured within the laminate by the FBG sensor as a function of time. The thermocouple signal is also shown as a reference.

At the beginning of the curing process, the strain was zero and the room temperature was of 27 $^{\circ}C$. After closing the autoclave, the temperature was increased to 70 $^{\circ}C$ in one hour. In this time interval, the temperature and the strain could not be measured by the FBG sensor, because the changes were too fast for the interrogation system to follow. Indeed, 14 minutes were required to acquire a FBG sensor value due to the low scanning speed of the laser/wavelength meter system over the gratings wavelength range. During the dwell, the strain was positive in the composite because the thermal expansion of the aluminum base-plate (corresponding to about 1000 $\mu\varepsilon$) was partially transferred to the composite. Then the strain decreased as a result of the polymer cross-linking. During the second heating ramp, the strain further decreased since the thermal expansion coefficient of the composite is negative. In the post-curing phase, the strain still decreased because of the polymer cross-linking. Finally, in the cooling down the composite expanded due to its negative thermal expansion coefficient. After the curing process, the residual internal strain was of 340 $\mu\varepsilon$. The temperature measurement from the FBG sensor followed the thermocouple values within 6%. The thermocouple is placed on the surface of the sample while the fiber sensor is embedded inside the laminate. This can result in a small temperature difference and can add to the maximum experimental errors of ±22.1 $\mu\varepsilon$ and ±2.4 $^{\circ}C$ calculated for the this FBG sensor [18].

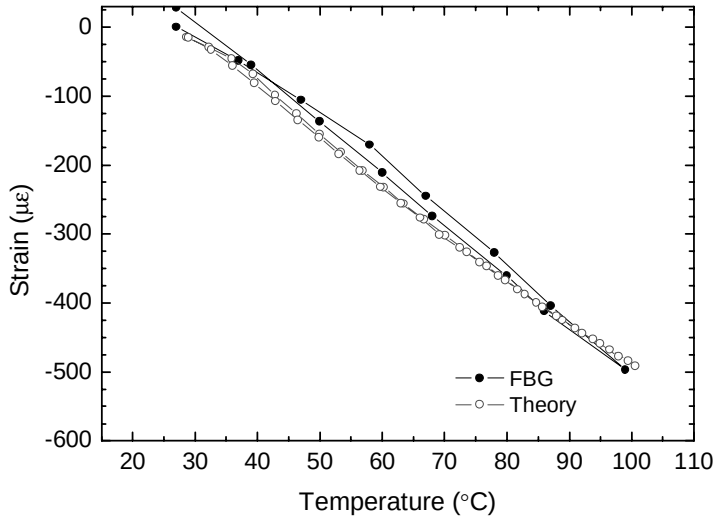

Figure 7: Thermal activation of the adaptive composite sample: strain measured by the FBG sensor and predicted by theory as a function of temperature.

After the curing process, activation of the SMA wires was performed by heating the composite sample in an oven up to $100^{\circ}C$. Figure 7 shows the recovery strain in the composite measured by the FBG sensor. The composite contracted when heated due to the combined effects of the negative thermal expansion and the recovery of the SMA wires above their transformation temperature. The experimental strain-temperature curve compared well with an elastic force balance analysis [3, 23].

4. CONCLUSIONS

In this paper, a sensor suitable for the simultaneous measurement of strain and temperature within a host composite material has been realized and tested. The sensor is formed by two FBGs, which are written in optical fibers with different dopants. A sensing element results with two Bragg gratings having peak wavelengths around 1550 nm of similar strain sensitivity but different response to temperature due to the dependence of the fiber thermo-optic coefficient on the core dopants and dopants concentration. FBGs in a germano-silicate fiber with 22 mol% GeO_2 and in a Fibercore PS1500 germanium-boron co-doped fiber were selected for building this sensing element. The temperature coefficients were different by 26%, resulting in an improved condition number with respect to similar works.

Strain and temperature of a Kevlar epoxy adaptive composite, in which several 150µm diameter NiTiCu shape memory alloy wires were embedded, are measured simultaneously using an embedded FBG sensor during the cure cycle. Finally, activation tests were performed on the composites by placing them in an oven up to 100 °C, and monitoring the strain and temperature. The composite contracted upon heating due to the recovery of the SMA wires above the transformation temperature. The experimental strain-temperature curve compared well with an elastic force balance analysis.

ACKNOWLEDGEMENTS

The authors would like to acknowledge the KAIST-EPFL exchange program for sponsoring Hyuk-Jin Yoon as a visiting graduate student at EPFL under the Swiss-Korean collaboration program. The work at KAIST is supported by Smart UAV Development Center.

REFERENCES

1. A.D. Kersey, M.A. Davis, H.J. Patrick, et al., “Fiber Grating Sensors”, Journal of Lightwave Technology, **15**, pp. 1442-1463, 1997.
2. J.A. Balta, V. Michaud, M. Parlinska, et al., “Adaptive composites with embedded NiTiCu wires”, Smart Structures and Materials 2001: Active Materials, 4333, pp. 377-386, Proceedings SPIE, 2001.
3. V. Michaud and J.-A. E. Månson, “Progress and design of composites with Embedded Shape memory Alloy wires”, Transactions of the Materials Research Society of Japan, **29**, pp. 3043-3048, 2004.
4. M.G. Xu, J.L. Archambault, L. Reekie, et al., “Discrimination between strain and temperature effects using dual-wavelength fibre grating sensors”, Electronics Letters, **30**, pp. 1085-1087, 1994.
5. J. Echevarria, A. Quintela, C. Jauregui, et al., “Uniform fiber Bragg grating first- and second-order diffraction wavelength experimental characterization for strain-temperature discrimination”, IEEE Photonics Technology Letters, **13**, pp. 696-698, 2001.
6. P.M. Cavaleiro, F.M. Araujo, L.A. Ferreira, et al., “Simultaneous measurement of strain and temperature using Bragg gratings written in germanosilicate and boron-codoped germanosilicate fibers”, IEEE Photonics Technology Letters, **11**, pp. 1635-1637, 1999.
7. B.O. Guan, H.Y. Tam, S.L. Ho, et al., “Simultaneous strain and temperature measurement using a single fibre Bragg grating”, Electronics Letters, **36**, pp. 1018-1019, 2000.
8. H.J. Patrick, G.M. Williams, A.D. Kersey, et al., “Hybrid fiber Bragg grating/long period fiber grating sensor for strain/temperature discrimination”, IEEE Photonics Technology Letters, **8**, pp. 1223-1225, 1996.
9. S.W. James, M.L. Dockney and R.P. Tatam, “Simultaneous independent temperature and strain measurement using in-fibre Bragg grating sensors”, Electronics Letters, **32**, pp. 1133-1134, 1996.
10. J. Jung, H. Nam, J.H. Lee, et al., “Simultaneous measurement of strain and temperature by use of a single-fiber Bragg grating and an erbium-doped fiber amplifier”, Applied Optics, **38**, pp.2749-2751, 1999.
11. X.K. Zeng and Y.J. Rao., “Simultaneous static strain, temperature and vibration measurement using an integrated FBG/EFPI Sensor”, Chinese Physics Letters, **18**, pp. 1617-1619, 2001.
12. H.K. Kang, D.H. Kang, C.S. Hong, et al., “Simultaneous monitoring of strain and temperature during and after cure of unsymmetric composite laminate using fibre-optic sensors”, Smart Materials and Structures, **12**, pp. 29-35, 2003.
13. L.A. Ferreira, F.M. Araujo, J.L. Santos, et al., “Simultaneous measurement of strain and temperature using interferometrically interrogated fiber Bragg grating sensors”, Optical Engineering, **39**, pp.2226-2234, 2000.
14. M. Song , S.B. Lee, S.S. Choi, et al., “Simultaneous measurement of temperature and strain using two fiber Bragg gratings embedded in a glass tube”, Optical Fiber Technology, **3**, pp. 194-196, 1997.
15. B.O. Guan, H.Y. Tam, H.L.W. Chan, et al., “Discrimination between strain and temperature with a single fiber Bragg grating”, Microwave and Optical Technology Letters, **33**, pp. 200-202, 2002.
16. X. Shu, Y. Liu, D. Zhao, et al., “Dependence of temperature and strain coefficients on fiber grating type and its application to simultaneous temperature and strain measurement”, Optics Letters, **27**, pp. 701-703, 2002.
17. O. Frazao, M.J.N. Lima and J.L.Santos, “Simultaneous measurement of strain and temperature using type I and type IIA fibre Bragg gratings”, Journal of Optics A-Pure Applied Optics, **5**, pp. 183-185, 2003.
18. P. Sivanesan, J.S. Sirkis, Y. Murata, et al., “Optimal wavelength pair selection and accuracy analysis of dual grating sensors for simultaneously measuring strain and temperature”, Optical Engineering, **41**, pp. 2456-2463, 2002.
19. G. Strang, *Linear algebra and its applications*, Harcourt Brace Jovanovich College Publishers, San Diego, 1988.
20. K. Oh, Y.G. Han, H.S. Seo, et al., "Compositional dependence of the temperature sensitivity in a long period grating imprinted on GeO_2-B_2O_3 co-doped core silica fibers", OSA Trends in Optics and Photonics, **33**, pp. 243-245, 2000.
21. S. Kannan, J.Z.Y. Guo and P.J. Lemaire, “Thermal Stability Analysis of UV-Induced Fiber Bragg Gratings”, Journal of Lightwave Technology, **15**, pp. 1478-1483, 1997.
22. J.M. Jewell, C. Askins and I.D. Aggarwal, “Interferometric method for concurrent measurement of thermo-optic and thermal expansion coefficients”, Applied Optics, **30**, pp. 3656-3660, 1991.
23. V. Michaud, J. Schrooten, M. Parlinska, et al., “Shape memory alloy wires turn composites into smart structures. Part II: manufacturing and properties”, Smart Structures and Materials 2002: Industrial and Commercial Applications of Smart Structures Technologies, 4698, pp. 406-415, Proceedings SPIE, 2002.